Numerical investigation of acoustic solitons

Bruno Lombard[a]*, Jean-François Mercier[b], and Olivier Richoux[c]

[a] LMA, CNRS, UPR 7051, Aix-Marseille Université, Centrale Marseille, F-13402 Marseille Cedex 20, France
[b] POEMS, CNRS/ENSTA/INRIA, UMR 7231, ENSTA ParisTech, 91762 Palaiseau, France
[c] LAUM, UMR 6613 CNRS, Université du Maine, 72085 Le Mans, France

Abstract. Acoustic solitons can be obtained by considering the propagation of large amplitude sound waves across a set of Helmholtz resonators. The model proposed by Sugimoto and his coauthors has been validated experimentally in previous works. Here we examine some of its theoretical properties: low-frequency regime, balance of energy, stability. We propose also numerical experiments illustrating typical features of solitary waves.

Key words: nonlinear acoustics, solitary waves, fractional derivatives.

1. INTRODUCTION

Solitons are nonlinear waves with large amplitude and constant profile, resulting from the balance between nonlinearity and dispersion [1]. In acoustics, the dispersion is too low compared with the nonlinearity to produce solitons. Thus additional geometric dispersion must be considered to observe acoustic solitons. It was the basis of a series of works of Sugimoto and coauthors [6,7], where the propagation of nonlinear acoustic waves was investigated in a tube connected with an array of Helmholtz resonators. A mathematical model was proposed, as well as a theoretical analysis and a comparison with experimental data.

Sugimoto's work was extended in two directions. In [3], a time-domain numerical model was proposed to incorporate efficiently the fractional derivatives, modelling linear viscothermic losses. In [5], comparisons with experimental results were proposed. It was shown that nonlinear attenuation in the resonators had also to be incorporated for describing accurately the experiments.

The goal of this paper is to analyse further Sugimoto's model with fractional derivatives and nonlinear attenuation. In the low-frequency regime, the evolution equations tend to a Korteweg–de Vries equation with an additional nonlinear term. The fractional model is transformed by means of a diffusive representation, which allows to analyse the energy balance and the stability of the model. Lastly, two sets of numerical experiments are proposed, showing that the waves have the typical features of solitary waves.

---

* Corresponding author, lombard@lma.cnrs-mrs.fr

2. FRACTIONAL MODEL

2.1. Sugimoto's equations

The configuration is depicted in ([3, fig. 2]). The wavelengths are much larger than the distance between two resonators, so that the latter are described by a continuous distribution. One-dimensional propagation is assumed. The velocity of gas u and the excess pressure in the resonators p satisfy equations

$$
\begin{cases}
\dfrac{\partial u}{\partial t} + \dfrac{\partial}{\partial x}\left(au + b\dfrac{u^2}{2}\right) = c\dfrac{\partial^{-1/2}}{\partial t^{-1/2}}\dfrac{\partial u}{\partial x} + d\dfrac{\partial^2 u}{\partial x^2} - e\dfrac{\partial p}{\partial t}, & \text{(1a)} \\[3mm]
\dfrac{\partial^2 p}{\partial t^2} + f\dfrac{\partial^{3/2} p}{\partial t^{3/2}} + gp - m\dfrac{\partial^2 (p)^2}{\partial t^2} + n\left|\dfrac{\partial p}{\partial t}\right|\dfrac{\partial p}{\partial t} = hu, & \text{(1b)}
\end{cases}
$$

see [5] for the expression of the coefficients. The PDE (1a) describes the right-going nonlinear wave propagation (a and b) in the tube. The losses in the tube are introduced by c (viscothermic losses at the wall) and by d (volume attenuation). The ODE (1b) describes the oscillations in the resonators, where the losses are introduced by f (viscothermic losses) and by n (jet loss due to the difference in inflow and outflow patterns). The coefficient m results from the nonlinearity in adiabatic relation in the cavity. Coupling between (1a) and (1b) is ensured by e and h. A fractional integral of order 1/2 (c) and a fractional derivative of order 3/2 (f) are introduced. These operators are non-local in time and amount to convolution products.

2.2. Low-frequency approximation

Under the hypothesis of weak nonlinearity, $\partial u/\partial x$ in (1a) is replaced by $-(1/a)\,\partial u/\partial t$ in the terms with coefficients b, c, and d. The resulting system is written in the (T, X) coordinates, where T is a non-dimensional retarded time, X is a nondimensional slow space variable:

$$
T = \omega\left(t - \dfrac{x}{a}\right), \qquad X = \varepsilon\,\omega\,\dfrac{x}{a}, \qquad \varepsilon = \dfrac{\gamma + 1}{2}\dfrac{u_{\max}}{a}, \tag{2}
$$

where $u_{\max}$ is the magnitude of the gas velocity at the initial time, ω is a characteristic wave frequency, and γ is the ratio of specific heats at constant pressure and volume. Introducing the reduced variables U and P

$$
U = \dfrac{1}{\varepsilon}\dfrac{\gamma + 1}{2}\dfrac{u}{a} = \mathcal{O}(1), \quad P = \dfrac{1}{\varepsilon}\dfrac{\gamma + 1}{2\gamma}\dfrac{p}{p_0} = \mathcal{O}(1), \tag{3}
$$

where p_0 is the pressure at equilibrium, one obtains the system

$$
\begin{cases}
\dfrac{\partial U}{\partial X} - U\dfrac{\partial U}{\partial T} = -\delta_R\dfrac{\partial^{1/2} U}{\partial T^{1/2}} + \beta\dfrac{\partial^2 U}{\partial T^2} - K\dfrac{\partial P}{\partial T}, & \text{(4a)} \\[3mm]
\dfrac{\partial^2 P}{\partial T^2} + \delta_r\dfrac{\partial^{3/2} P}{\partial T^{3/2}} + \Omega P - M\dfrac{\partial^2 P^2}{\partial T^2} + N\left|\dfrac{\partial P}{\partial T}\right|\dfrac{\partial P}{\partial T} = \Omega U. & \text{(4b)}
\end{cases}
$$

This system generalizes ([7], Eqs (2-5) and (2-6)) to the case of nonlinear processes in the resonators (terms with M and N). As shown in [6], β is negligible compared to δ_r and δ_R. We consider waves with characteristic frequencies much smaller than the natural frequency of the resonators ω_e, so that $\Omega = (\omega_e/\omega) \gg 1$. In this case, the dispersion analysis performed in [3] indicates that the viscothermal

losses are small. Moreover, the volume of the resonators is large compared to that of the necks, so that $M \ll N$ is neglected. Consequently, the low-frequency regime $\Omega \gg 1$ yields the simplified system

$$
\begin{cases}
\dfrac{\partial U}{\partial X} - U \dfrac{\partial U}{\partial T} = -K \dfrac{\partial P}{\partial T}, & \text{(5a)} \\[3mm]
\dfrac{\partial^2 P}{\partial T^2} + \Omega P + N \left| \dfrac{\partial P}{\partial T} \right| \dfrac{\partial P}{\partial T} = \Omega U. & \text{(5b)}
\end{cases}
$$

From (5b), one obtains

$$
P \;=\; U - \frac{1}{\Omega} \frac{\partial^2 U}{\partial T^2} - \frac{N}{\Omega} \left| \frac{\partial U}{\partial T} \right| \frac{\partial U}{\partial T} + \mathscr{O}\left(\frac{1}{\Omega^2} \right). \tag{6}
$$

Injecting (6) in (5a) gives:

$$
\frac{\partial U}{\partial X} + K \frac{\partial U}{\partial T} - U \frac{\partial U}{\partial T} = \frac{K}{\Omega} \frac{\partial^3 U}{\partial T^3} + \frac{2KN}{\Omega} \left| \frac{\partial U}{\partial T} \right| \frac{\partial^2 U}{\partial T^2} + \mathscr{O}\left(\frac{1}{\Omega^2} \right).
$$

Neglecting the second-order terms in $1/\Omega$ and introducing the new unknown $V = U - K$, leads to the PDE

$$
\frac{\partial V}{\partial X} - V \frac{\partial V}{\partial T} = \frac{K}{\Omega} \frac{\partial^3 V}{\partial T^3} + \frac{2KN}{\Omega} \left| \frac{\partial V}{\partial T} \right| \frac{\partial^2 V}{\partial T^2}. \tag{7}
$$

When nonlinear attenuation in the resonators is neglected ($N = 0$), Eq. (7) recovers the Korteweg–de Vries equation in ([6], (2-35)), which allows the propagation of solitons. Solitons are also expected to exist for small N values, but with a decrease of the amplitude.

3. DIFFUSIVE MODEL

3.1. Evolution equations

A diffusive approximation of the nonlocal in time fractional operators in Eq. (1) is followed here [4]. The half-order integral of a function $w(t)$ can be written as

$$
\frac{\partial^{-1/2}}{\partial t^{-1/2}} w(t) = \frac{1}{\sqrt{\pi}} \int_0^t (t - \tau)^{-1/2} w(\tau)\, d\tau = \int_0^{+\infty} \phi(t, \theta)\, d\theta \simeq \sum_{\ell=1}^N \mu_\ell \phi_\ell(t), \tag{8}
$$

where the diffusive variable ϕ satisfies the local-in-time ordinary differential equation

$$
\frac{\partial \phi}{\partial t} = -\theta^2 \phi + \frac{2}{\pi} w. \tag{9}
$$

In Eq. (8), $\phi(t, \theta_\ell) = \phi_\ell(t)$; μ_ℓ and θ_ℓ are the weights and nodes of the quadrature formula. Their computation is detailed in [5]. A similar derivation is applied to the 3/2 derivative in Eq. (1), involving the diffusive variable ξ. Injecting these diffusive approximations in Eq. (1) yields the following system of evolution equations

$$
\begin{cases}
\dfrac{\partial u}{\partial t} + \dfrac{\partial}{\partial x} \left(au + b \dfrac{(u)^2}{2} \right) = c \displaystyle\sum_{\ell=1}^N \mu_\ell \phi_\ell + d \dfrac{\partial^2 u}{\partial x^2} - eq, \\[3mm]
\dfrac{\partial p}{\partial t} = q, \\[3mm]
\dfrac{\partial q}{\partial t} = \dfrac{1}{1 - 2mp} \left(hu - gp - f \displaystyle\sum_{\ell=1}^N \mu_\ell \left(-\theta_\ell^2 \xi_\ell + \dfrac{2}{\pi} q \right) + 2m(q)^2 - n|q|q \right), \\[3mm]
\dfrac{\partial \phi_\ell}{\partial t} - \dfrac{2}{\pi} \dfrac{\partial u}{\partial x} = -\theta_\ell^2 \phi_\ell, \qquad \ell = 1 \cdots N, \\[3mm]
\dfrac{\partial \xi_\ell}{\partial t} = -\theta_\ell^2 \xi_\ell + \dfrac{2}{\pi} q, \qquad \ell = 1 \cdots N.
\end{cases} \tag{10}
$$

In the hypothesis of weak nonlinearity, one has $1 - 2mp > 0$ [5]. The $(3 + 2N)$ unknowns are

$$\mathbf{U} = (u, p, q, \phi_1, \cdots, \phi_N, \xi_1, \cdots, \xi_N)^T.$$ (11)

Then the nonlinear system (10) can be written in the form

$$\frac{\partial}{\partial t}\mathbf{U} + \frac{\partial}{\partial x}\mathbf{F}(\mathbf{U}) = \mathbf{S}(\mathbf{U}) + \mathbf{G}\,\frac{\partial^2}{\partial x^2}\mathbf{U}.$$ (12)

3.2. Energy balance

Based on the system (10), we define

$$\mathscr{E} = \frac{1}{2}\int_{\mathbb{R}}\left(u^2 + \frac{eg}{h}p^2 + \frac{e}{h}q^2\,(1 - 2mp) + \frac{\pi}{2}\frac{ef}{h}\sum_{\ell=1}^{N}\mu_\ell\,\theta_\ell^2\,\xi_\ell^2\right)dx.$$ (13)

Assuming smooth solutions (no shock) and $c = 0$, then one obtains

$$\frac{d\mathscr{E}}{dt} = -\int_{\mathbb{R}}d\left(\frac{\partial u}{\partial x}\right)^2 dx - \frac{\pi}{2}\int_{\mathbb{R}}\frac{ef}{h}\sum_{\ell=1}^{N}\mu_\ell\left(\frac{\partial \xi_\ell}{\partial t}\right)^2 dx - \int_{\mathbb{R}}\frac{en}{h}q^2\left(|q| - \frac{m}{n}q\right)dx.$$ (14)

To ensure that $\mathscr{E} > 0$ in (13), one needs $\mu_\ell > 0$ and $1 - 2mp > 0$. The first condition is enforced by the optimization with constraint of positivity used to determine the weights [5]. The second condition is satisfied in the hypothesis of weak nonlinearity (see the sentence after system (10)). The energy decreases in (14) if $\mu_\ell > 0$ and $m < n$. The first condition has been examined. The second one is satisfied, since $m/n = \frac{\gamma - 1}{2}\frac{BL_e}{V}$, where BL_e is the volume of the neck, and V is the volume of the resonator [5]. By assumption, this ratio is smaller than 1.

Let us finally examine the other assumptions. With shocks, the wave motion is irreversible and additional terms of dissipation must be accounted for in (14). On the other hand, the hypothesis $c = 0$ is not physical but is required for technical purpose: up to now, we have not found an energy if $c \neq 0$.

3.3. Stability analysis

The system (12) is solved by a splitting technique [5]: one successively solves the PDE

$$\frac{\partial}{\partial t}\mathbf{U} + \frac{\partial}{\partial x}\mathbf{F}(\mathbf{U}) = \mathbf{G}\,\frac{\partial^2}{\partial x^2}\mathbf{U}$$ (15)

and the ODE

$$\frac{\partial}{\partial t}\mathbf{U} = \mathbf{S}(\mathbf{U})$$ (16)

with adequate time steps. Here we examine the stability of both stages. First, $\partial\mathbf{F}/\partial\mathbf{U}$ has real eigenvalues $\{a + bu, 0^{2N+2}\}$ and is diagonalizable. Consequently, (15) is hyperbolic when $\mathbf{G} = \mathbf{0}$. In practice, $\mathbf{G}$ introduces a parabolic regularization, and the problem remains well-posed.

We have no general result about the stability of (16). But some partial results have been obtained, depending on the dissipation mechanisms considered:
 (i) nonlinear processes in the resonators ($m \neq 0$ or $n \neq 0$), no fractional losses ($c = f = 0$). Then the eigenvalues of $\mathbf{T} = \partial\mathbf{S}/\partial\mathbf{U}$ are $\{0, \lambda^+, \lambda^-\}$. If $m \leq n/2$, then $\mathfrak{Re}(\lambda^\pm) \leq 0$ and (16) is stable. This constraint is satisfied when the volume of the resonators is large compared to that of the necks, which is the case in practice (a similar argument has been used in previous sections);

(ii) linear processes in the resonators ($m = n = 0$), viscothermic losses in the waveguide ($c \neq 0$) but not in the resonators ($f = 0$). The eigenvalues of $\mathbf{T}$ are $\left\{0, \pm i\sqrt{g + eh}, -\theta_\ell^2\right\}$ hence (16) is stable;

(iii) linear processes in the resonators ($m = n = 0$), viscothermic losses ($c \neq 0$ and $f \neq 0$). Then 0 and $-\theta_\ell^2$ are simple eigenvalues of $\mathbf{T}$ ($\ell = 1 \cdots N$). Moreover, assuming positive weights $\mu_\ell > 0$ and nodes $\theta_\ell > 0$, and ordering the nodes as $0 < \theta_1 < \theta_2 < \cdots < \theta_N$, then N other eigenvalues λ_ℓ are real negative and satisfy:

$$\lambda_N < -\theta_N^2 < \cdots < -\theta_{\ell+1}^2 < \lambda_\ell < -\theta_\ell^2 < \cdots < \lambda_1 < -\theta_1^2 < 0. \tag{17}$$

In the limit case $f = 0$, the two remaining eigenvalues λ_{2N+2} and λ_{2N+3} are equal to the imaginary eigenvalues of case (ii): $\pm i\sqrt{g + eh}$. If $f \neq 0$, numerical tests indicate that these two eigenvalues are complex conjugates with a negative real part.

From cases (ii) and (iii), it follows that the spectral radius of the Jacobian satisfies $\rho(\mathbf{T}) = |\lambda_N| > \theta_N^2 \gg 1$. As a consequence, (16) must be solved by an implicit scheme [5]. We conjecture that this stiffness of $\mathbf{T}$ still holds for nonlinear processes in the resonators ($m \neq 0$ or $n \neq 0$) and for the general case (10). This justifies the splitting strategy.

4. NUMERICAL RESULTS

In this part, we examine whether the solution of the Sugiomoto's model (1) has the typical features of solitons. In test 1, one investigates the dependence of the velocity upon the amplitude of the forcing. In test 2, we simulate the interaction between two waves.

4.1. Study of the velocity in terms of the amplitude

The physical and geometrical parameters are given in [5]. Two values of the resonators height are considered: $H = 2$ cm and $H = 7$ cm, modifying the resonance angular frequency of the Helmholtz resonators (ω_e in section) and the parameters K and N in (7). The waves are generated by imposing the value of the velocity in (10) at $x = 0$. A Gaussian profile with amplitude A is chosen for this purpose:

$$u(0,t) = \begin{cases} A e^{-\left(\frac{t-t_0}{\tau}\right)^2} & \text{if } 0 \leq t \leq 2t_0, \\ \\ 0 & \text{otherwise.} \end{cases} \tag{18}$$

The central frequency is $f_0 = 1/t_0 = 650$ Hz. The standard deviation τ is chosen so that $u(0,0) = u(0,2t_0) = A/1000$. A set of 10 receivers is distributed uniformly on the computational domain. Seismograms are built from the time signals stored. The positions of the maximal value of u at each receiver is detected and allows to estimate the celerity $\mathcal{V}$ of the wave. An example for $H = 7$ cm and $A = 100$ m/s is given in Fig. 1a. After a transient regime (offsets 0 and 1), a smooth structure emerges despite the nonsmoothness of the evolution equations (10). The amplitude of the wave decreases along propagation, due to the loss mechanisms. Lastly, small amplitude waves are observed before the main wave front.

The same procedure is followed by varying A from 10 to 100 m/s. The evolution of $\mathcal{V}$ in terms of A is illustrated in Fig. 1b. The linear increase of $\mathcal{V}$ with A is clearly observed. Greater values of $\mathcal{V}$ are obtained for smaller value of H. These two observations confirm the theoretical analysis performed in [7].
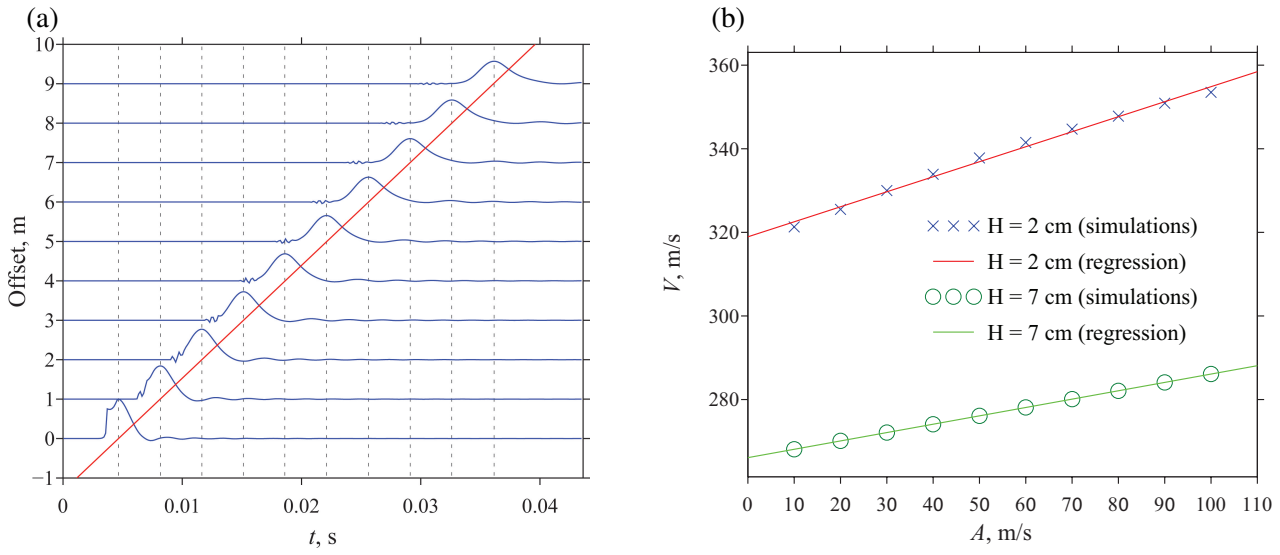
Fig. 1. Test 1. (a) example of the seismogram. The vertical dotted lines represent the location of the maximum at each receiver. The inclined red line denotes the trajectory of these maxima; its slope yields the velocity of the wave. (b) velocity of the waves in terms of the forcing amplitude.

4.2. Interaction of two solitons

A pulse with small amplitude followed by a taller pulse are generated. Due to its higher amplitude, the latter travels faster, allowing an interaction between the two soliton waves (Fig. 2). In the inviscid case (a), we observe that the two waves interact in a manner analogous to classical solitons [2]: after the waves separate, each one has again the form of a solitary wave, though shifted in location from where they would be without interaction (denoted by crosses). When the attenuation mechanisms are accounted for (b), a similar observation can be done, even if the observation is not so clear due to the smoothing of waves.
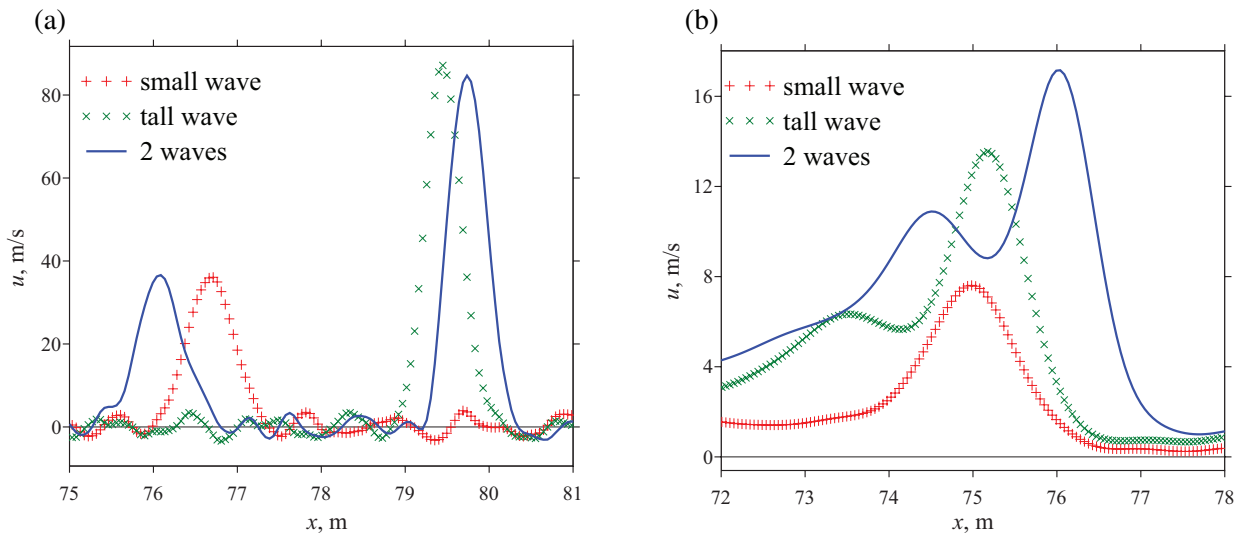

Fig. 2. Test 2, with $H = 7$ cm. Snapshots of u after the interaction of two waves: (a) without dissipation, (b) with attenuation.

5. CONCLUSIONS

In this contribution, we have studied some properties of the full Sugimoto's model with nonlinear attenuation. Besides practical applications mentioned in [6], the main interest of this model is to test the properties of acoustic solitons in a configuration that can be studied both experimentally and theoretically. Numerical experiments have allowed to examine situations difficult to reproduce experimentally. They have shown that typical features of solitons are maintained despite the nonlinear attenuation mechanisms.

ACKNOWLEDGEMENTS

REFERENCES

1. Engelbrecht, J., Fridman, V., and Pelinovski, E. *Nonlinear Evolution Equations*. Longman, Harlow, 1988.
2. LeVeque, R. J. and Yong, D. H. Solitary waves in layered nonlinear media. *SIAM J. Appl. Math.*, 2003, **63**, 1539–1560.
3. Lombard, B. and Mercier, J. F. Numerical modeling of nonlinear acoustic waves in a tube with Helmholtz resonators. *J. Comput. Phys.*, 2014, **259**, 421–443.
4. Matignon, D. An introduction to fractional calculus. In *Scaling, Fractals and Wavelets* (Abry, P., Goncalves, P., and Lévy Véhel, J., eds). ISTE-Wiley, 2008, 237–273.
5. Richoux, O., Lombard, B., and Mercier, J. F. Generation of acoustic solitary waves in a lattice of Helmholtz resonators. *Wave Motion*, 2015, **56**, 85–99.
6. Sugimoto, N. Propagation of nonlinear acoustic waves in a tunnel with an array of Helmholtz resonators. *J. Fluid. Mech.*, 1992, **244**, 55–78.
7. Sugimoto, N., Masuda, M., Yamashita, K., and Horimoto, H. Verification of acoustic solitary waves. *J. Fluid. Mech.*, 2004, **504**, 271–299.

Akustiliste solitonide numbriline uurimine

Bruno Lombard, Jean-François Mercier ja Olivier Richoux

Akustilised solitonid võivad tekkida, kui suure amplituudiga helilaine levib läbi Helmholtzi resonaatorite komplekti. Eelmistes töödes oleme eksperimentaalselt valideerinud Sugimoto ja tema kaasautorite välja-töötatud mudelit. Käesolevas artiklis kontrollime mõnd selle mudeli teoreetilist omadust: madala sageduse režiimi, energia tasakaalu ja stabiilsust. Samuti esitame numbriliste eksperimentide tulemusi, kus on näidatud, milline on üksiklainete kiiruse ja amplituudi vaheline seos ning millisel juhul üksiklained käituvad kui klassikalised solitonid.